ISSN 2706-655X Vol.6, Issue 5: 117-125, DOI: 10.25236/IJFET.2024.060517

Minimal Impact of Manipulator When Grabbing Load

Jiajun Tang[1,a], Junlin Huang[1,b], Wei Luo[1,c], Dawei Zhang[1,d], Muhan Wu[1,e], Yu Cheng[1,f,*], Wei Lu[1,g]

[1]School of Mechanical and Electrical Engineering, Guilin University of Electronic Technology, Guilin, Guangxi, China
[a]820912216@qq.com, [b]1791512826@qq.com, [c]3140514436@qq.com, [d]2672836044@qq.com, [e]1514655367@qq.com, [f]cheng19971223@qq.com, [g]lujunqi2001@163.com
[*]Corresponding author

Abstract: *This paper studies the stability control strategy of a seven-degree-of-freedom space manipulator carrying a massive load, and uses computer simulation to analyze the minimum impact force of the manipulator when grasping the load. It is found that the impact force generated by the robot arm is affected by the arm length, mass, power and other related factors, among which the mass is the most affected, about 10% higher than other parameters. In addition, it is found in the experiment that the heavier the mass of the robot arm, the greater the impact; Through this experimental simulation, the minimum impact of the robot arm when grasping the load is between 2-4, and the working efficiency of the robot arm is not reduced. This shows that the manipulator can improve its efficiency by reducing the impact when grasping the load.*

Keywords: *Manipulator, Load, Manipulator Trajectory, Minimum Impact force*

1. Introduction

In the complex working environment, the manipulator needs to have the characteristics of high precision, light weight, low power consumption and low energy consumption. In dynamic analysis, arm flexibility must be included to reflect the actual motion trajectory [1]. The parts of the manipulator are connected by moving pairs, and the clearance and friction are the key factors affecting the performance and accuracy. This paper focuses on these factors [2]. So the development of high-precision robot manipulator arms becomes particularly important [3]. Although the size of the space robot arm is large, small deformation can lead to significant errors, so its design needs to take into account accuracy and efficiency. Mechanism is the core of mechanical system, and its kinematic characteristics directly affect the functional and structural complexity [4].

Experts at home and abroad have conducted extensive research on manipulators. Huang Jian, Liu Yanchuo, Zhao Xinhu, and others compared the running paths of multiple sets of space manipulators, summarized and compared relevant data, and studied the optimal operation trajectory [5]. Gao Juanjuan, Gao Jingfang, Hou Tiantian, and Liu Fucai used a PD closed-loop iterative learning control algorithm to track the manipulator's trajectory, established related models, and conducted simulation experiments [6]. Xia Wei analyzed the main role of manipulators in space exploration, focusing on the tracking accuracy of the manipulator's end, established a two-degree-of-freedom manipulator model with gaps, and analyzed the influence of gravity on the manipulator's end trajectory [7].Yang Feifei, Wang Cong, Zeng Wei, and others studied the learning performance of a manipulator based on system control, constructing a manipulator model and issuing different commands, concluding that mode control can improve manipulator performance [8]. Zhao Jieliang and Yan Shaoze studied various factors affecting the manipulator, particularly the change in control accuracy under alternating thermal and cold radiation in space, and improved related dynamic modeling issues [9]. JianLin et al. studied the effect of meshing stiffness instability on a two-stage gear transmission system, analyzing the impact of time-varying meshing stiffness parameters on the stability of the planetary transmission system, finding that instability can be controlled by adjusting the contact ratio and meshing phase, and verified the numerical solution accuracy [10]. Huang Ping and Ge Xinsheng studied the dynamic characteristics of manipulators, proving through experiments their stability and passivity, though the complexity of the robotic arm's operation resulted in less accurate results [11].

ISSN 2706-655X Vol.6, Issue 5: 117-125, DOI: 10.25236/IJFET.2024.060517

In this paper, the minimum impact force of a manipulator is studied. Based on the conservation of momentum method, the identification method of inertia parameters with known and unknown initial momentum is derived by kinematic analysis and dynamic modeling. The objective function of the optimal excitation is obtained by using the basic parameter set method, and optimized by the pattern search optimization algorithm. Finally, the advantages of the optimal excitation are verified by comparing the two paths through simulation experiments.

2. Current Status of Manipulators and Impact Calculation Methods

2.1 Manipulator Composition

Three coordinate methods can be selected to describe the motion of the multi-space manipulator system, which are relative coordinate method, absolute coordinate method and natural coordinate method [12]. The natural coordinate method (NCF) was founded by Garcia de Jalon and Bayo [13], and gave an efficient solution method that satisfies real-time simulation. The natural coordinate method selects the base point and unit vector for each element, and its Cartesian component constitutes the natural coordinates of the element. The constraint equation is formed through rigid body conditions and hinge constraints. Only Cartesian parameters are used, without rotation parameters, also known as complete Cartesian coordinates [14]. The natural coordinate method of differential algebraic equations has the advantages of moderate coordinate number, simple constraint equation, linear Jacobian matrix, constant mass matrix, etc., but because of the complexity of modeling, the use of rotation Angle and torque concepts, the development of slow. In China, Liu Yanzhu and Hong Jiazhen conducted the research of multi-rigid body system earlier.

The dynamic model of the manipulator is established by combining the joint composed of DC servo motor and flexible planetary gear drive system with the rigid arm. Considering the time-varying meshing stiffness caused by the change of tooth number, the time-varying mesh stiffness is treated as a constant in the simulation calculation, and the nonlinear factors such as friction and backlash are ignored. It is found that planetary gear transmission has an important effect on the dynamic behavior of the robot arm, but the establishment and solution of planetary gear dynamic model still need further research.

The study of manipulator kinematics focuses on the mapping relationship between joint space and task space, including forward and inverse kinematics. For the redundant manipulator, the forward kinematics method is the same as that of the non-redundant manipulator, but the inverse kinematics method is different. The dynamics of a flexible multi-body system focuses on the influence of the deformation of the flexible body on the dynamic characteristics of the system. Different from the "multi-body" dynamics of a multi-body system, the coupling effect between the elastic deformation of the object and the motion of the rigid body is studied [15]. The issues that need to be considered for modeling are:

(1) The model is reasonably simplified. By coupling flexible objects with a wide range of rigid bodies, the parts with greater impact on the system dynamics are highlighted, while the parts with less impact are ignored.

(2) The influence of large-scale motion on the dynamic characteristics of flexible objects in the discrete process is studied. Floating platform frame method, rotating coordinate method and absolute node coordinate method are commonly used in modeling of robotic arm, among which the absolute node coordinate method is the most commonly used and accurate, and is suitable for the description of various robot arm models [16].

2.2 Dynamic Equation of Space Manipulator

When the robotic arm is operating, suppose it rotates with x degrees of freedom, and its rotation is Q_i (i=2,...n), and the system center point is used O_j as a reference base value for operation in space [17], and a fixed The origin of the base is assumed to be connected to the base W^j (j=1,...n), and the system moves in a plane along the orbit. The dynamic formula is shown in Equation 1:

ISSN 2706-655X Vol.6, Issue 5: 117-125, DOI: 10.25236/IJFET.2024.060517

$$\sum_{n=1}^{i}\left(\vartheta r_n * w_n r_n + \vartheta \mu_n j_n \mu_n\right) - \sum_{j=1}^{i} \vartheta \theta_n v_n - \vartheta r_i * S_i = Q \tag{1}$$

Among them is the driving force v_n for turning dumplings, which is the impact force received S_i when the load is captured. If the rectangular $n_{ij} = \sum_{T=n}^{j} n_T$ array Z and the vector v are introduced, the relationship between the absolute turning angle $n_{ij} = \sum_{T=n}^{j} n_T$ and the relative angle $\mu = \left(\mu_1, \ldots \mu_n\right)^z$ is:

$$\vartheta = -z^z \mu \tag{2}$$

And the relative system centroid vector is expressed as:

$$b_i = \sum_{j=1}^{n} g_{ij} \delta_i^j \tag{3}$$

Among them $g_{ij} = \frac{-\sum_{}^{n} m_r d_{rj}}{m_{1n}}$, $g_{ij} = g_{jl} + d_{ij}\left(i, j = 1, \ldots n\right)$, take (2) and (3) into equation (1) and get the rectangular matrix dynamic equation:

$$ZM\left(\vartheta\right)Z^Z \vartheta - Zc\left(\vartheta, \dot{\vartheta}\right) = \delta + ZB\left(\vartheta\right)F_n \tag{4}$$

Among them, Fn is the value of the impact force on the mechanical arm.

2.3 The Influence of Friction When the Mechanical Arm Grabs the Load

Through the analysis of the specific manipulator, it is found that about 20% of the driving torque is used to overcome the friction resistance [18]. Reducing friction torque can be achieved by improving lubrication conditions, improving machining accuracy and designing effective transmission systems, and friction compensation technology can also be used to optimize system performance [19]. The friction calculation method is as follows:

$$f_n = P\delta^n + W\delta \tag{5}$$

In this formula, f represents the friction force received by the robotic arm, P represents the rate of movement of the robotic arm, δ which is the force generated by collision friction, and W represents the resistance generated during friction. For two objects in contact, the radius Are ri and rj respectively, then

$$P = \frac{6}{5\left(a_i + a_j\right)}\left[\frac{r_i r_j}{r_i + r_j}\right]^{\frac{1}{2}} \tag{6}$$

Material parameter a_i, a_j is

$$a_n = \frac{1 - t_n^2}{S_n}, (n = i, j) \tag{7}$$

In Equation 7, t is the running time of the object, and S is the running speed of the space manipulator of the object. The contact force has a nonlinear relationship with the deformation without considering the contact energy loss, but the low-speed collision force can be reduced [20]. Solid models of joint shell, planetary gear reducer and rigid arm need to be created for modeling. Joint dynamics

ISSN 2706-655X Vol.6, Issue 5: 117-125, DOI: 10.25236/IJFET.2024.060517

modeling is completed in ADAMS, and dynamic characteristics of transmission unit are ignored in simplified models.

2.4 Manipulator Gear Power Calculation

Based on the simplified joint model, a refined joint model is established considering the dynamic characteristics of the transmission device, and the influence of planetary gear transmission on the dynamic characteristics is analyzed. The flexible and rigid reduced arm joint models are basically the same, mainly considering the flexibility of the arm [21]. The angular displacement function is commonly used as a higher-order polynomial function:

$$\delta_i(r) = x_0 + x_1 r + x_2 r + x_3 r + x_4 r \tag{8}$$

Then, each coefficient xj is determined by known conditions. Suppose that during the operation of the robotic arm, the angle of the end of the arm at x=0 is δ_t, and the angle of xt at the planning end time is δ_t. In order to meet the continuity and stability of motion, the above variables need to meet the following conditions at the same time:

$$\begin{cases} \delta(r_0) = \delta_s \\ \delta(r_x) = \delta_x \\ \dot{\delta}(r_0) = 0 \\ \dot{\delta}(r_x) = 0 \end{cases} \tag{9}$$

The inertial parameters of the manipulator change with its motion. Using known structure and link inertia parameters, the center of mass and inertia of the whole mechanical arm can be accurately calculated, and then the change of impact force can be understood [22-24]. Recursive least square method is used for online identification, and parameters are updated in real time through recursive algorithm to ensure that the accuracy meets the requirements [25-26].

3. Simulation Experiment of Manipulator

3.1 Research Purpose

In this paper, the software was used to analyze the driving torque of joint 1 and joint 2 when the robot arm is grasping with friction and without friction, and the influence of friction on the robot arm was studied. The designed microsimulation system mainly considers gravity, gravity of structural components and eccentric bending moment and other load factors [27].

3.2 Manipulator Design

The manipulator designed in this paper has three joints, one flip joint and two expansion joints. The expansion joints have the same structure. The robotic arm flip joint is composed of a motor, a harmonic reducer, a flange, a bearing seat, an angular contact ball bearing, a root rotating shaft, an in-position switch, etc [28].

3.3 Force of the Robotic Arm

Table 1: Force on the boom

Name	Minimum force	Maximum force
Equivalent stress	0	25.14
Principal stress	-3.54	27.23
Displacement	0	0.741

Since the support point is located in arm 3, arm 1 needs to bear the force of expansion joint 2. The mechanical arm rod is made of carbon fiber, which requires rigidity and cost consideration. The pipe with inner diameter of 100 and outer diameter of 110 is selected. The force of arm 1 is shown in Table

ISSN 2706-655X Vol.6, Issue 5: 117-125, DOI: 10.25236/IJFET.2024.060517

1:

3.4 Mechanical Arm Force Calculation

In the motor motion of the manipulator, the maximum angular speed of the root node rotation is 1.5/s. Taking into account the adjustment accuracy of 0.1, the maximum Angle error of the arm rod 1 should be 0.1. The motor driving torque is designed according to the root node motor.

The minimum angular acceleration of the robotic arm is

$$\lambda_{\min} = \varphi^2 / 2\delta = 2.5^2 / 2.2 = 9.37^\circ / s^2 = 0.3rad / s^2 \tag{10}$$

The maximum angular speed represents the maximum angular error. At this time, the torque generated during movement is:

$$N_{\text{flip}} = W_{\text{flip}}\lambda \tag{11}$$

During the flip motion, the subsequent system only offloads the gravity of the entire arm 3 and the expansion joint 2. Assume that the unloading efficiency is 85%, that is, 15% of the gravity of arm 3 is not unloaded. According to these conditions, the moment of inertia of the W axis of rotation is:

$$W_{\text{flip}} = \frac{N_1 r_1^2}{2} + \frac{N_2 r_2^2}{2} + N_2 d_2^2 + \left(\frac{N_3 r_3^2}{2} + N_3 d_3^2 \right) * 0.1 + \frac{2}{3} N \tag{12}$$

4. Experimental Analysis of Manipulator

4.1 Various Parameters of the Robotic Arm

The inertial parameter identification and simulation experiments are carried out, and the effects of two kinds of manipulator trajectories are compared. The motion of trajectory one on only two axes may result in insufficient deformation of the manipulator. To solve this problem, the excitation design is optimized, the excitation signal is optimized by parametric method, and the optimization effect is verified by simulation experiment. The identification results of inertial parameters are shown in Table 2 and Figure 1:

Table 2: Manipulator parameters

Parameter	Truth value	Track one	The optimal value
Quality	500	436	437
Centroid	34	31.24	33.72
Rotational inertia	153.2	143.78	147.24
Product of inertia	135	127	134.5
Mechanical axis	124	127	123.14

It can be seen from Figure 1 that the identification effect is more obvious on the axis where the centroid of the manipulator changes greatly, and the identification result is better than other axial parameters under the most exciting trajectory.

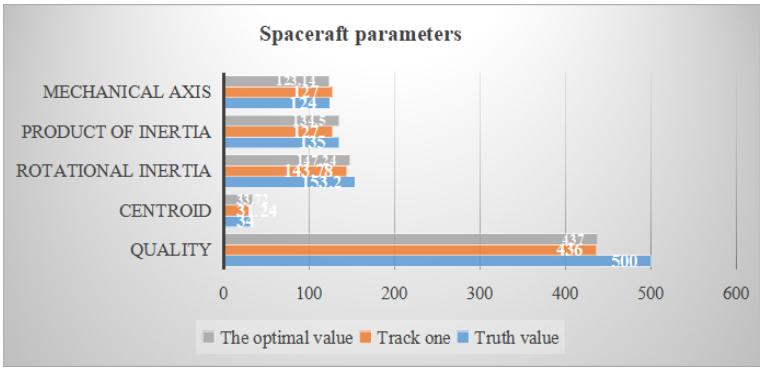

Figure 1: Manipulator parameters

ISSN 2706-655X Vol.6, Issue 5: 117-125, DOI: 10.25236/IJFET.2024.060517

4.2 Influence of Various Parameters of the Manipulator on the Impact Force

In this experiment, 3 manipulators with different parameters are designed. The parameters are shown in Table 3. The impact force of each manipulator when grasping different loads is shown in Figure 2:

Table 3: Space manipulator operating parameters

Parameter	Robot arm 1	Control group 1	Control group 2
Arm length	15	18	20
Weight	55	67	73
Operating rate	145.5	162.3	184.9
Power	325	428	496

Table 4: Impact force

Manipulator/weight mass	40(kg)	60(kg)	80(kg)	100(kg)
Robot arm 1	18	23	27	33
Control group 1	27	31	37	42
Control group 2	26	29	31	34

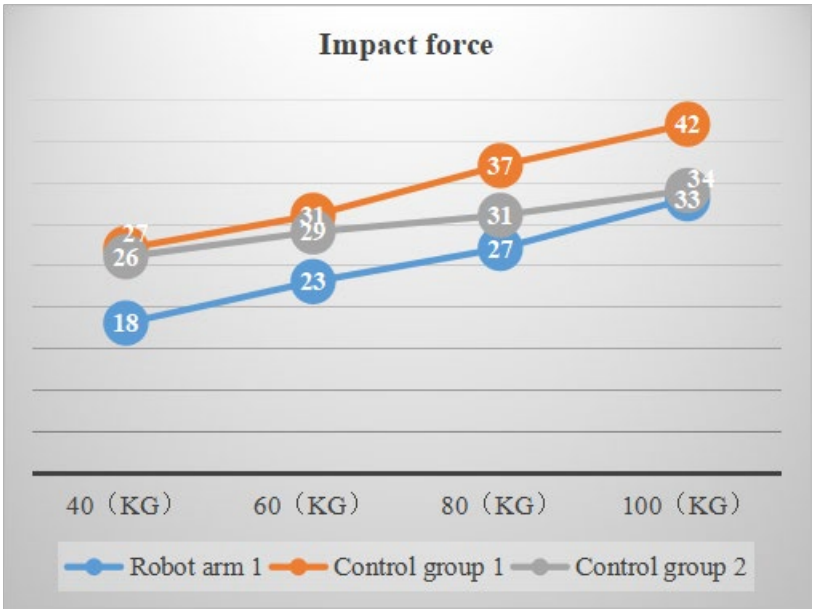

Figure 2: Impact force

It can be clearly seen from Figure 2 and Table 3 and Table 4 that the impact force of the robotic arm increases as the mass of its load object increases. The heavier the object loaded, the greater the impact force it causes. Length and operating speed all affect the impact force caused by the load of the robotic arm.

4.3 Optimization of Robotic Arm Parameters

In order to test the minimum impact force of the load of the manipulator, this article changes the relevant parameters of the manipulator, and the manipulator under different parameters to determine the optimal direction of the space manipulator. After the parameter changes, the impact force changes are shown in Figure 3:

Table 5: Space manipulator parameter changes

Arm length	17	19	21
Weight	57	60	63
Operating rate	150	175	200
Power	350	390	420

ISSN 2706-655X Vol.6, Issue 5: 117-125, DOI: 10.25236/IJFET.2024.060517

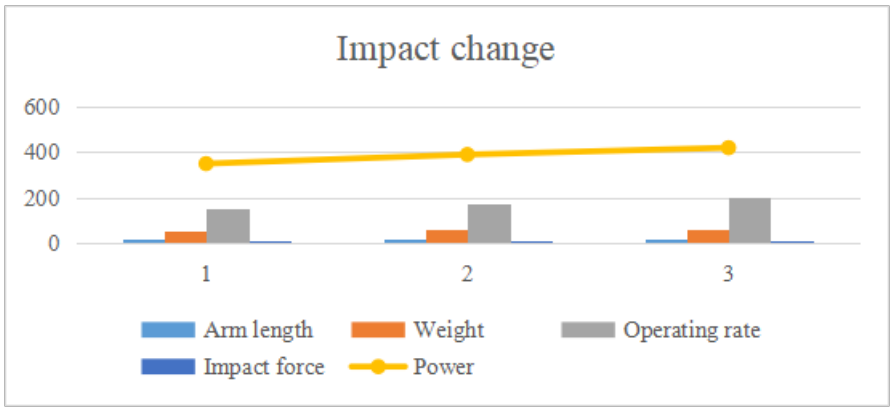

Figure 3: Impact force of robotic arm after changing parameters

From Figure 3 and Table 5, we can clearly see that after changing the relevant parameters of the manipulator, the impact force caused by the load of the manipulator is reduced. In this experiment, we increased the length of the manipulator. Corresponding changes have been made to the quality and operating power of the manipulator, which effectively reduces the impact force of the manipulator.

4.4 Optimal Impact Force Range of Manipulator

In order to determine the minimum impact force range of the manipulator under load, we conducted many experiments through experiments and finally determined the relevant range of the impact force of the manipulator under load, as shown in Figure 4:

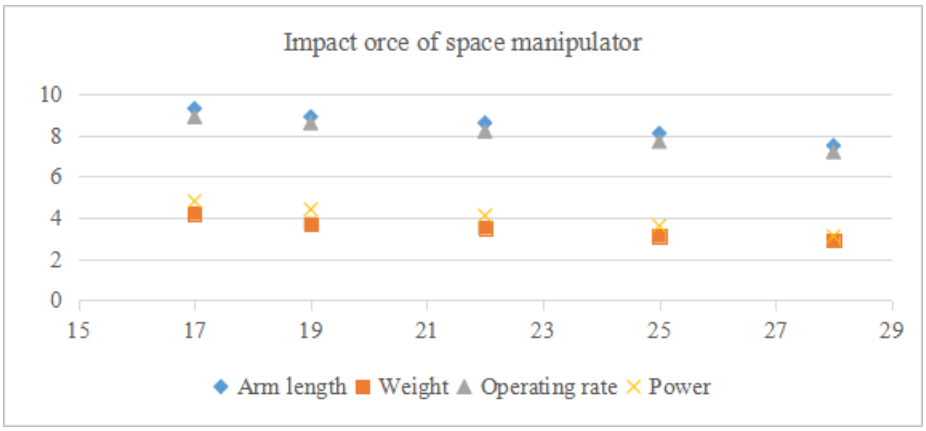

Figure 4: Impact force of manipulator

From Figure 4, we can see that in this experimental test, the minimum impact force of the manipulator load is about 3.5, which is much smaller than the minimum impact force of the manipulator before optimization. However, due to the limitations of tools and methods, the data of this test has certain limitations. In the subsequent research experiments, we must design more reasonable data, and through more scientific methods, the results of the experiment can present better results.

5. Conclusions

The space flexible mechanical arm is composed of multiple arm rods, which are connected by hinges. Due to parts processing errors, assembly errors and wear during use, gaps in the hinges of the mechanism are unavoidable. The existence of the gap will cause the manipulator arm to vibrate violently, which will seriously affect the dynamic performance of the manipulator arm, reduce the work accuracy of the manipulator arm, and cause its task to fail. When considering gravity, the friction between the hinges of the manipulator has a serious impact on the manipulator.

The design of a manipulator must first ensure its high reliability. Therefore, although mathematical simulation is used in the initial stage of its design and development, only when it is verified on a physical or semi-physical simulation platform can the designer study the design object at close range.

ISSN 2706-655X Vol.6, Issue 5: 117-125, DOI: 10.25236/IJFET.2024.060517

Dynamics issues during execution. The design object participates in the simulation process in the physical way of hardware, and the test result is perfect, true and credible. At the same time, due to the particularity of the space environment, it is very difficult to completely reflect the various factors that may appear in the actual operation process through the mathematical model. Semi-physical simulation can be comprehensive under various environmental conditions and initial conditions. Investigate the working conditions of each device of the robotic arm, shorten the development cycle, and have high reliability. Therefore, the development of a semi-physical simulation test system for a manipulator and exploring the motion control and stability of the manipulator have important theoretical and practical value. At the same time, the experience of semi-physical simulation of the manipulator can be applied to the dynamic control of large-scale deployable structures in the future.

Acknowledgement

This work was supported by the National College Student Innovation and Entrepreneurship Training Program Project (202410595031).

References

[1] Huang Jian, Liu Yanchuo, Zhao Xinhu. Research on the path of space manipulator [J]. Mechanical Engineering and Automation, 2018, No. 208(03):84-85+88.
[2] Gao Juanjuan, Gao Jingfang, Hou Tiantian, et al. Space manipulator ground setup and space application iterative learning control [J]. Manned Spaceflight, 2015, 021(001):83-90.
[3] Xia Wei. Research on modeling and trajectory tracking control of manipulator with gap space considering the influence of gravity [D]. 2017, 003(013):183-190.
[4] Liu Fucai, Xia Wei, Lan Hui, et al. FOTSMC trajectory tracking control of a space manipulator with hinge gap under different gravity environments [J]. High Technology Communications, 2018, 28(Z2): 65-73.
[5] Liu Fucai, Xia Wei, Qin Li, et al. Trajectory tracking control of PDμ-SMC manipulator with inter-hinge gap space under different gravity conditions [J]. High Technology Letters, 2017, 003(4): 152-155+182.
[6] Wang Kang, Liang Changchun, Lin Yuncheng, et al. Design and research of telescopic rod self-reconfigurable space manipulator system[C]. Manned Aerospace Editorial Department, 2015, 4(14):182-185.
[7] Zhao Jieliang; Yan Shaoze; The influence of thermal alternating environment on the on-orbit operation of space manipulator[C]. The 10th National Multibody Dynamics and Control and the 5th National Aerospace Dynamics and Control Conference Abstracts. 2017, 007(004):152-155.
[8] Huang Ping, Ge Xinsheng. Attitude control stability of space manipulator based on energy method [J]. International Aerospace Science, 2017, 005(001):P. 45-53.
[9] Sui Tingting, Ma Xiao, Guo Jian, et al. Research on Obstacle Avoidance Dynamics Control of Redundant Space Manipulator [J]. Computer Simulation, 2019, 036(005):349-353.
[10] Gao Juanjuan, Gao Jingfang, Hou Tiantian, et al. Space manipulator ground setup and space application iterative learning control [J]. Manned Spaceflight, 2015, 021(001):83-90.
[11] Li Taitai, Li Wenxin, Duan Fuwei, et al. Parametric inverse kinematics solution of joint angle of offset space manipulator [J]. Machine Tool & Hydraulics, 2018, 46(09):47-51.
[12] Xin Pengfei, Rong Jili, Yang Yongtai. Research on Space Manipulator Vibration Suppression Based on PSO Optimization Algorithm [J]. Manned Spaceflight, 2016, 22(001):23-28.
[13] Zhang Ruifen. A control strategy based on fuzzy recurrent neural network for a space manipulator subject to external disturbances [J]. Mechanical & Electrical Engineering, 2017, 34(001):62-67.
[14] Yu Xiaoyan, Chen Li. Uncertain Parameters and Bounded Interference Free-floating Flexible Space Manipulator Based on Velocity Observer Singular Perturbation Robust Control and Vibration Suppression [J]. Journal of Vibration and Shock, 2015, 003(14):90-97.
[15] Liang Changchun, Zhang Xiaodong, Tang Zixin, et al. Inhibition of sudden changes in speed caused by joint failure of space manipulator [J]. Journal of Astronautics, 2016, v.3 (01):51-57.
[16] Wu Liangkai, Wang Tao, Wang Chunli, et al. Dynamic Modeling and Simulation Analysis of 3D Space Manipulator [J]. Mechanical Engineer, 2017, 001(013):150-152.
[17] Liu Fucai, Liu Lin, Xu Zhiying. Simulation Research on Singular Perturbation Fuzzy PID Control of Flexible Joint Space Manipulator [J]. High Technology Letters, 2019, 29(7):661-667.
[18] Huang Xiaoqin, Chen Li. Integral sliding mode neural network adaptive control for floating-based space manipulators with joint torque output dead zone and external interference [J].

ISSN 2706-655X Vol.6, Issue 5: 117-125, DOI: 10.25236/IJFET.2024.060517

Chinese Journal of Computational Mechanics, 2018, 35(06):713-718.
[19] Mo Yang, Zhang Dawei, Tang Ling, et al. Space manipulator assisted large-mass capsule docking impedance control method [J]. Manned Spaceflight, 2016, 22(001):126-131.
[20] Xin Xingshan, Chen Li. Observer-based decentralized adaptive fuzzy control and flexible vibration feedback control for flexible space manipulators[C]. The 15th National Nonlinear Vibration and the 12th National Nonlinear Dynamics and Motion Stability Collection of abstracts of academic conferences on sex. 2015, 02(01):136-139.
[21] Liu Fucai, Li Qian, Liang Lihuan, et al. Adaptive backstepping sliding mode control of space manipulator trajectory tracking in different gravity environments [J]. High Technology Letters, 2015, 001(4):384-392.
[22] Li Yuqi, Shao Zhufeng, Tian Sihui, et al. Analysis and evaluation of unloading rate of space manipulator zero-gravity simulation device based on hanging wire counterweight [J]. Robot, 2016, 38(3):293-300.
[23] Yu Xiaoyan, Chen Li. Uncertain parameters and bounded interference free-floating flexible space manipulator based on velocity observer robust control and vibration suppression for singular perturbation [J]. Journal of Vibration and Shock, 2015, 001(014):85 -92.
[24] Jia Qingxuan, Li Tong, Chen Gang, et al. Sensitivity analysis of factors influencing the motion reliability of space manipulator based on multi-layer mapping model [J]. Chinese Journal of Mechanical Engineering, 2017, 001(11):123-125.
[25] Liang Jie, Chen Li, Liang Pin. Rigid-flexible coupling dynamics simulation of space manipulator and wavelet-based fuzzy neural network control [J]. Manned Spaceflight, 2015, 021(003):286-294.
[26] Huang Xiaoqin, Chen Li. Dynamic surface control of anti-dead zone and friction of floating-based space manipulator [J]. Journal of Huazhong University of Science and Technology (Natural Science Edition), 2018, 46(4): 74-79.
[27] Jensen Raufelder. Modeling Analysis of Attitude Perception of Engineering Manipulator Supporting Wireless Communication and Internet of Things [J]. Kinetic Mechanical Engineering, 2021, 2(2): 18-26.
[28] Chen H, Yang Y, & Shao C. Multi-task learning for data-efficient spatiotemporal modeling of tool surface progression in ultrasonic metal welding [J]. Journal of Manufacturing Systems, 2021, 58, 306-315.